

Title	Microstructure Characterization of Cu <sub>6</sub> Sn <sub>5</sub> -based Intermetallic Compounds at Solder Matrix and Relevant Solder Joints
Author(s)	Gao, Feng; Nishikawa, Hiroshi; Takemoto, Tadashi
Citation	Transactions of JWRI. 2005, 34(2), p. 57-61
Version Type	VoR
URL	<a href="https://doi.org/10.18910/12170">https://doi.org/10.18910/12170</a>
rights	
Note	

*Osaka University Knowledge Archive : OUKA*

<https://ir.library.osaka-u.ac.jp/>

Osaka University

# Microstructure Characterization of $\text{Cu}_6\text{Sn}_5$ -based Intermetallic Compounds at Solder Matrix and Relevant Solder Joints<sup>†</sup>

GAO Feng \*, NISHIKAWA Hiroshi \*\*, and TAKEMOTO Tadashi \*\*\*

## Abstract

*The microstructures of intermetallic compounds at the interface and dispersed in the solder matrix were characterized in this paper. Two sorts of solders, Sn3.5Ag and Sn3.5Ag0.3Co were selected to examine the interfacial reaction with the Cu substrate. In the Sn3.5Ag0.3Co solder matrix, the ternary Sn-Cu-Co IMC was detected, which indicated that the additives exhibit high affinity with the Sn atoms. The IMC composition on the solder side is almost the same as the ones distributed within the solder matrix, which means that the formation of IMC at this side is related closely to the solder microstructure. On the other hand, much lower additive concentrations were observed on the Cu side (or  $\text{Cu}_3\text{Sn}$  phase after aging). The non-homogeneous characteristic of IMC was suggested owing to the non-uniform concentration distribution of additives, that is, the IMCs morphology at the interface seemed quite different. The faceted and elongated shape was observed at the solder side, while the nearly rounded shape seen at the Cu side.*

**KEY WORDS:** (Lead-free solder), (Intermetallic compounds), (Morphology), (Additive)

## 1. Introduction

Nowadays, the development of lead-free solders has been explored extensively owing to the environmental concerns [1-2]. As compared with the conventional Sn-Pb electronics, the employment of lead-free solders and components etc. will definitely result in more complex interactions during manufacturing. In the meanwhile, more fundamental reliability challenges will be encountered in future to achieve novel miniaturized and higher performance electronic devices. Therefore, to ensure the high reliability of electronic devices, it is quite essential to obtain a better understanding of solder/component interfacial reactions. In particular, the intermetallic compounds play a key role in electronic packaging. The formation of intermetallic compounds at the interface is the prerequisite condition to accomplish the connection between solder and components. However, the morphology, thickness and chemical composition of intermetallic compounds will affect the mechanical properties of solder joint significantly [3-5]. Thus, it will be necessary to observe the evolution of intermetallic compounds, not only at the interface, but also within the solder matrix.

Basically, the Sn-Ag and Sn-Cu solders and their derivatives have been regarded as the most promising lead-free solders to replace the conventional Sn-Pb solder. It has been reported that the additive Co into the Sn3.5Ag solder could maintain the shear strength after an aging process, and also result in the refined microstructure of the solder matrix [6]. Furthermore, Takemoto et al. has found that the erosion rate of stainless tank can be

depressed as a result of the effects of Co addition in Sn-based lead-free solders [7]. Thus in this paper, two sorts of solders, say, Sn3.5Ag and Sn3.5Ag0.3mass%Co (hereafter, the two sorts of solders will be merely referred as SA and SA-Co, respectively) were selected to react with the Cu substrate. The microstructure characteristics of intermetallic compounds were examined by SEM and EPMA, etc.

## 2. Experimental

Before the soldering process, the Cu substrate pad was degreased in ethanol and then dipped in 10 vol. % NaOH solution for 30 s. Two sorts of solders, namely, SA, SA-Co, were placed on the surface of the Cu pad with the commercial flux. The soldering tests were performed at 250°C from 1 to 60s. Some of samples were subjected to an aging process at 150°C for 504h. The microstructures of cross sections were then observed using SEM. In order to reveal the morphology of IMC at different view angles, the remaining solder was etched away with 13 vol. %  $\text{HNO}_3$  + 87 vol. % distilled water solution. The component elements of intermetallic compounds were measured by EPMA. And the crystal microstructure was determined by XRD.

## 3. Results

### 3.1 Cross-section observation

**Fig. 1** depicts the cross-sectioned microstructure of intermetallic compounds after soldering at 250°C for 1 and 60s respectively. Apparently, as compared with the SA/Cu couple, the SA-Co/Cu couple exhibits larger IMC

<sup>†</sup> Received on November 7, 2005

\* Foreign Guest Researcher

\*\* Assistant Professor

\*\*\* Professor

Transactions of JWRI is published by Joining and Welding Research Institute, Osaka University, Ibaraki, Osaka 567-0047, Japan

growth rate, in particular, during the short soldering time. After the prolonged reflow time, the coarsening behavior of IMC grains for the SA/Cu couple is significant, while is not severe for the SA-Co/Cu couple. Consequently, the surface roughness of the IMC for the SA/Cu couple tends to be larger than that of SA-Co/Cu couple. The porous structure of the IMC for the SA-Co/Cu couple is suggested, since some area within the interfacial product region is occupied by “voids”, as marked in Fig. 1.

The chemical compositions of intermetallic compounds distributed at the solder joint interface, as

well as the solder matrix, were measured by EMPA. Three typical sites, that is, site 1, 2 and 3 indicated in Fig. 1(b) were selected to determine the element concentrations of the intermetallic compounds. In the mean time, the “void” structure was identified as a Sn-rich phase. The results are displayed in Table 1. Some amount of Co addition is detected in the intermetallic compounds both at the solder/Cu interface and within the solder matrix. The striking phenomenon is that the IMC composition at site 1 is quite different from that at site 2, especially the Co additive concentration.

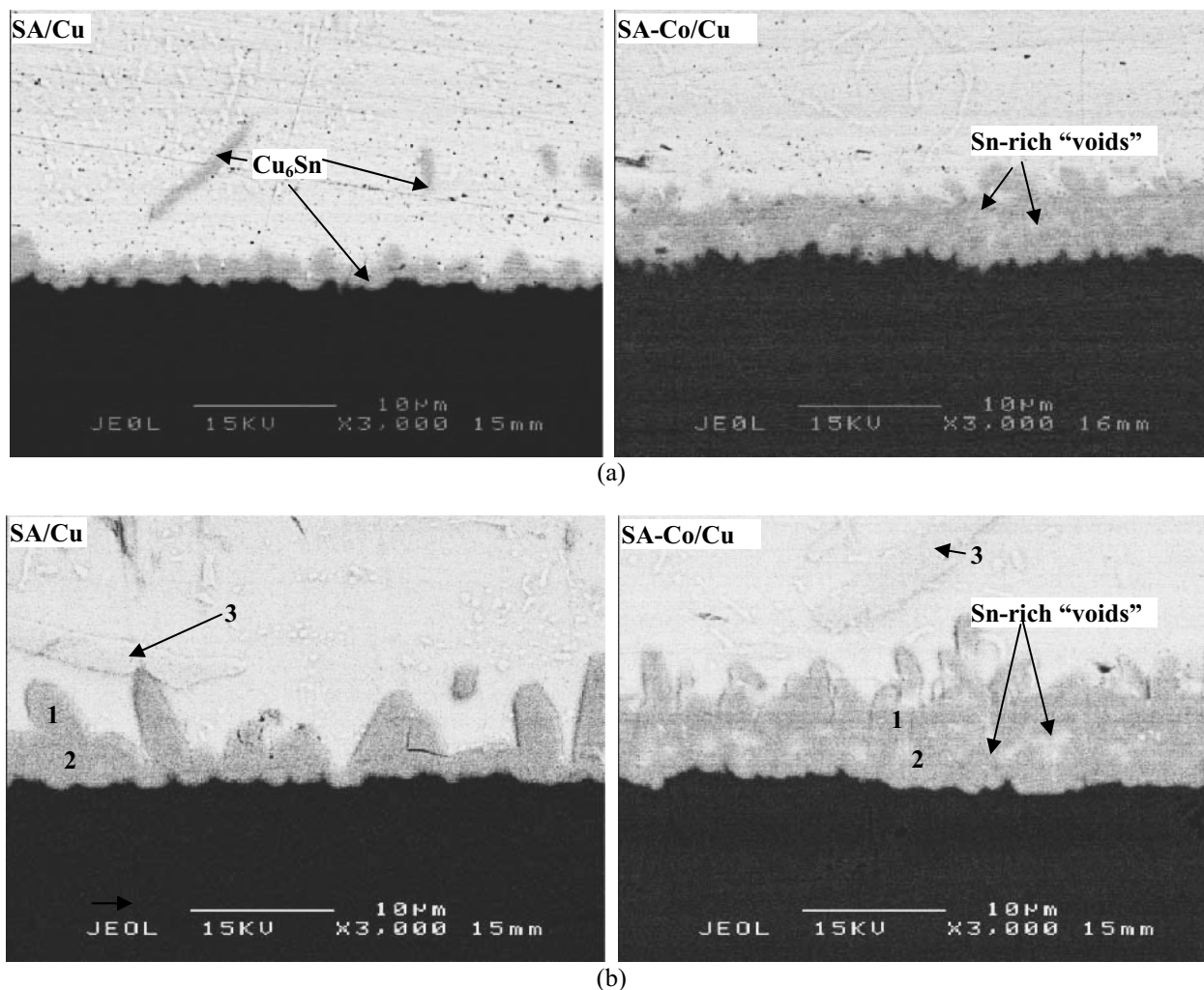


Fig. 1 The micrographs of IMCs at the solder/Cu joint soldered at 250°C for: (a) 1s; (b) 60s, respectively.

Table 1 The chemical compositions of IMC at the solder/Cu interface and solder matrix (atom %).

Reaction couple	Sn	Cu	Ag	Co	Phases	
SA/Cu	1	44.9	54.5	0.6	0.0	$\text{Cu}_6\text{Sn}_5$
	2	42.8	56.8	0.4	0.0	$\text{Cu}_6\text{Sn}_5$
	3	47.3	52.5	0.2	0.0	$\text{Cu}_6\text{Sn}_5$
SA-Co/Cu	1	47.8	43.4	0.2	8.6	$(\text{Cu}, \text{Co})_6\text{Sn}_5$
	2	46.3	52.3	0.1	1.3	$(\text{Cu}, \text{Co})_6\text{Sn}_5$
	3	46.9	46.1	0.1	6.9	$(\text{Cu}, \text{Co})_6\text{Sn}_5$
	Void	81.3	18.2	0.0	0.5	Sn-rich phase

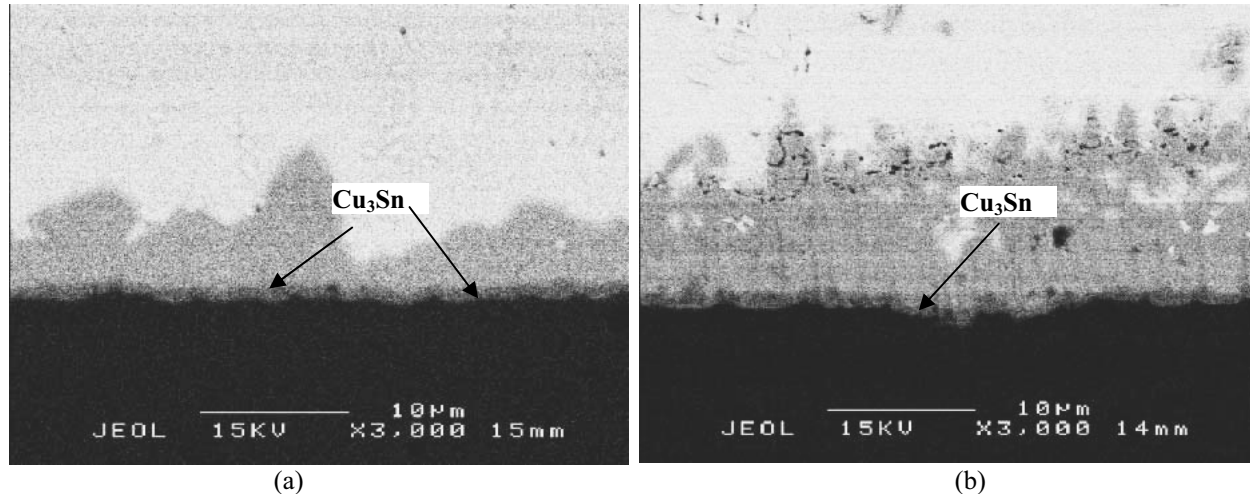


Fig. 2 The micrographs of intermetallic compounds after aging at 150°C for 504h: (a) SA/Cu couple; (b) SA-Co/Cu couple.

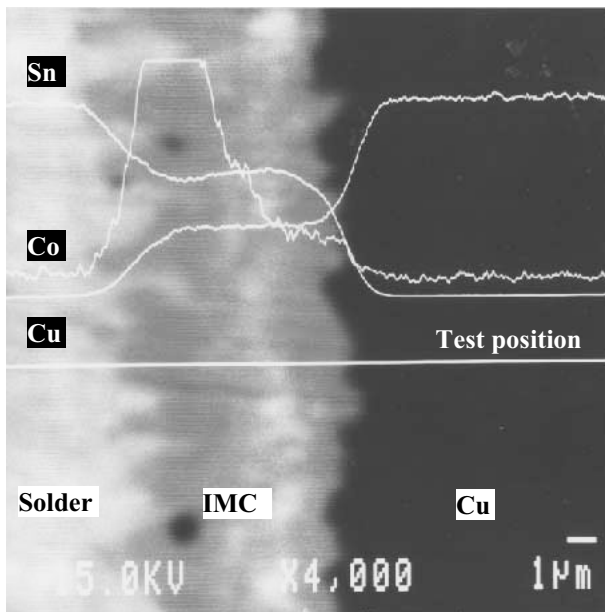


Fig. 3 Line analysis featuring the two distinct areas of the  $(\text{Cu}, \text{Co})_6\text{Sn}_5$  IMC between SA-Co and Cu.

That is, the Co concentration at the solder matrix side is much higher than that at the Cu side. It should be noticed that the Co concentration of intermetallic compounds dispersed in the solder matrix shows almost the same value as that of the upper IMC layer at the solder/Cu interface. This consistency will be an important sign to study the formation mechanism of IMC between SA-Co and Cu substrates.

After aging at 150°C for 504h, the coarsening behavior of IMC for the SA/Cu couple continues and the morphology of IMC tends to be flat. While for the SA-Co/Cu couple, the “voids” entrapped within the IMC region dwindle and this leads to a more compact microstructure, as shown in Fig. 2(b). For both SA/Cu and SA-Co/Cu couples, the  $\text{Cu}_3\text{Sn}$  phase is generated due to the reaction  $\text{Cu}_6\text{Sn}_5 + \text{Cu} \rightarrow \text{Cu}_3\text{Sn}$ . However, it seems

that the formation of  $\text{Cu}_3\text{Sn}$  phase for SA-Co/Cu is greatly depressed. Fig. 3 illustrates the line analysis results using EPMA, which further demonstrates the non-homogeneous characteristic, namely, the duplex structure of intermetallic compounds for the SA-Co/Cu diffusion couple. In order to study the crystal microstructure of IMCs, the XRD technique was employed after a deep-etching treatment to remove the solder matrix. Fig. 4 shows the XRD patterns of IMCs for SA/Cu and SA-Co/Cu couples, respectively. Obviously, the incorporation of Co into the intermetallic compounds does not cause the alternation of crystal microstructure. That is, the IMC formed between SA-Co and Cu can be suggested as  $\text{Cu}_6\text{Sn}_5$ -based. Actually, since the  $\text{Cu}_6\text{Sn}_5$  has high Co and Ni solubility [8], it has sometimes been labeled the  $(\text{Cu}, \text{Co})_6\text{Sn}_5$  phase.

### 3.2 Top-view observation

After the deep-etching, the IMC morphology of top-view is exposed, as depicted in Figs. 5-6. The  $\text{Cu}_6\text{Sn}_5$  IMC for SA/Cu couple exhibits typical rounded shape morphology. Some nano-size particles are observed on the surface of IMC grains and have been suggested as  $\text{Ag}_3\text{Sn}$  phase [9]. Apparently the IMC grains experienced significant ripening process, and grew continuously with the prolonged reaction time. However, for the SA-Co/Cu couple, the IMC morphology is quite different. The more striking phenomenon is that the morphology of the IMC adjacent to the solder matrix is also not the same as that of the inner IMC area, namely, at the Cu side, as shown in Fig. 6 (a) and Fig. 6 (b).

The upper IMC area for the SA-Co/Cu couple exhibits finer morphology, which indicates that that part of the IMC does not undergo the conventional coarsening behavior. A faceted elongated shape is suggested here. At the inner IMC area, a larger size IMC is detected in lateral directions and the elongated growth is depressed. In the mean time, the morphology of the IMC tends to be more rounded.

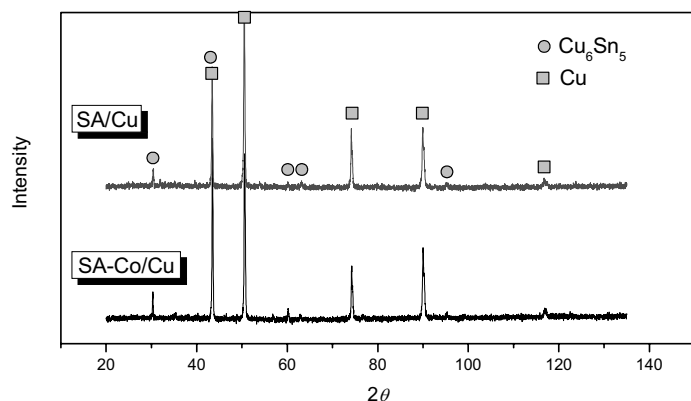


Fig. 4 XRD patterns of IMCs for SA/Cu and SA-Co/Cu couples.

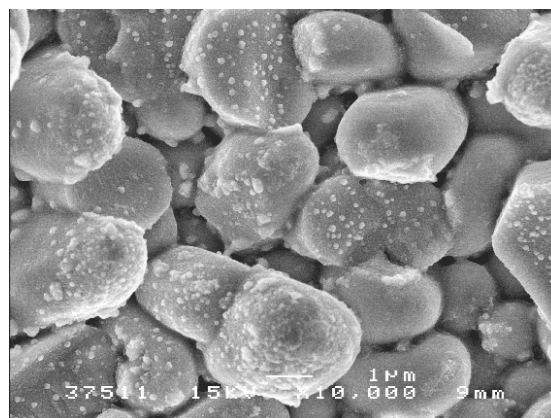


Fig. 5 Top-view of IMC for SA/Cu couple soldered at 250°C for 60s.

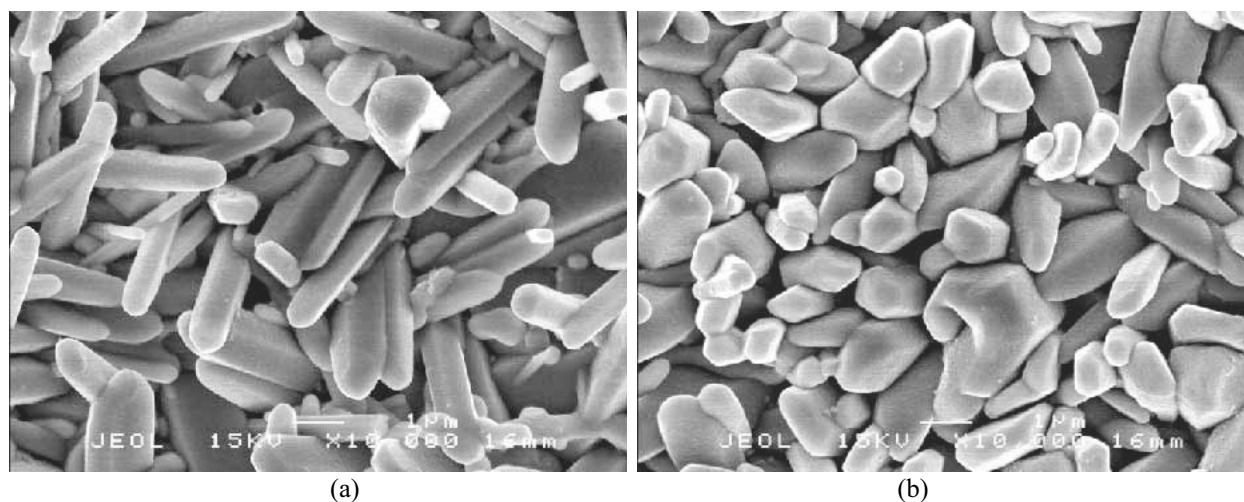


Fig. 6 Different IMC morphology of  $(\text{Cu, Co})_6\text{Sn}_5$  due to the Co concentration: (a) upper IMC area on the solder side; (b) Inner IMC area on Cu side.

### 3.3 Analysis

The involvement of additive Co into the intermetallic compound formation may be attributed to the affinity relationship between additive Co and Sn atoms [10]. Based on the thermodynamic models, the affinity of Sn/Co and Sn/Cu couples can be estimated. That is, the affinity of the Sn/Co couple is stronger than that of the Sn/Cu, as plotted in Fig. 7. The detail of thermodynamic models utilized here will be found in the literatures [11-12].

As a consequence, the higher affinity of Sn/Co may be reason why the addition Co can be traced in the  $\text{Cu}_6\text{Sn}_5$ -based IMC in the solder matrix. On the other hand, the higher affinity of Sn/Co couple will also restrain the additive Co to take part in the interfacial reaction at the beginning, since in a short reaction time, the diffusion of Cu from the substrate is quite fast into the liquid solder to trigger the interfacial reaction.

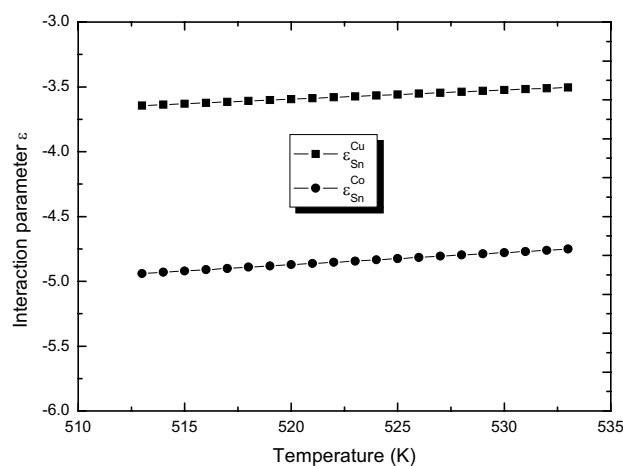


Fig. 7 The comparison of the affinity for Sn/Cu and Sn/Co couples.

After a longer reaction time, the diffusion of Cu will slow down and the growth rate of  $\text{Cu}_6\text{Sn}_5$  phase will decrease as well. With a lower growth rate, the nucleation mechanism will become more dominant. The higher affinity of Sn/Co can reduce the critical nucleation energy, because the so-called short range ordered microstructure may be generated in the solder matrix. The upper IMC layer will be created based on the nucleation on the surface of inner IMC grains. Thus the high solubility at the upper IMC layer will be possible, while the morphology will be slight different from the inner IMC layer owing to its formation mechanism and subsequent different Co concentration.

#### 4. Conclusions

Based on the observation of IMCs formed within the solder matrix and the solder/Cu interface, the following conclusions may be formulated:

- (1) The reaction products formed by SA/Cu and SA-Co/Cu couples are all  $\text{Cu}_6\text{Sn}_5$ -based. However, for the SA-Co/Cu couple, higher Co solubility in  $\text{Cu}_6\text{Sn}_5$  adjacent to the solder matrix is detected than that on the Cu side. The  $\text{Cu}_6\text{Sn}_5$  IMC is also found in the SA-Co solder matrix, which contains almost the same concentration of additive Co as the upper IMC layer located at the SA-Co/Cu interface.
- (2) For the interfacial products, a typical rounded shape of IMC formed between SA and Cu is observed, and dramatic coarsening behavior leads to the ripening of large size grains and shrinking of small size grains. For the SA-Co/Cu couple, the morphology of IMC at upper area is quite different from that at inner area. That is, a faceted and elongated shape of IMC is formed at upper area, while nearly rounded and coarse grains are found at inner area. The difference of IMC morphology may be attributed to the formation mechanism at different soldering stages.

#### Acknowledgement

The financial support through Japan Society for the Promotion of Science (JSPS) is greatly acknowledged.

#### References

- 1) M. Abteu, G. Selvaduray, Mater. Sci. Eng. R., Vol.27 (2000) pp. 95-141.
- 2) T. Laurila, V. Vuorinen, J.K. Kivilahti, Mater. Sci. Eng. R., Vol. 49, No. 1-2 (2005) pp. 1-60.
- 3) Y.C. Chan, A.C.K. So, J.K.L. Lai, Mater. Sci. Eng. B., Vol. 55, No. 1-2 (1998) pp. 5-13.
- 4) P.L. Tu, Y.C. Chan, J.K.L. Lai, IEEE Transactions on Advanced Packaging, Vol. 24, No. 2 (2001) pp. 197-205.
- 5) T.Y. Lee., et al., J. Mater. Res., Vol. 17, No. 2 (2002) pp. 291-301.
- 6) I.E. Anderson, J.C. Foley, B.A. Cook, J. Harringa, R.L. Terpstra, O. Unal, J. Electron. Mater., Vol. 30, (2001) pp.1050-1059.
- 7) T. Takemoto, T. Uetani, M. Yamazaki, Solder. Surf. Mt. Tech., Vol. 16 (2004) pp. 9-15.
- 8) C.-H. Lin, S.-W. Chen, C.-H. Wang, J. Electron. Mater., Vol. 31, No. 9 (2003) pp. 907-915.
- 9) D.Q. Yu, L. Wang, C.M.L. Wu, C.M.T. Law, J. Alloy. Compd., Vol. 389 (2005) pp.153-158.
- 10) F. Gao, T. Takemoto, H. Nishikawa, A. Komatsu, in Proceedings of 7<sup>th</sup> IPC/JEDEC Inter. Conf. Electron. Assembly and packaging, CD edition, Frankfurt, Germany, Oct. 2005.
- 11) A.R. Miedema, P.F. Chatel, F.R. Boer, Physica B., Vol. 100 (1980) pp.1-28.
- 12) K.-C. Chou, CALPHAD, Vol. 19 (1995) pp. 315-325.